OPEN ACCESS
IOP Publishing
Measurement Science and Technology
Meas. Sci. Technol. **31** (2020) 077001 (5pp)
https://doi.org/10.1088/1361-6501/ab78c1

Technical Note

Characterisation of a deep-ultraviolet light-emitting diode emission pattern via fluorescence

Mollie McFarlane and Gail McConnell

Department of Physics, University of Strathclyde, SUPA, Glasgow, U.K

E-mail: mollie.mcfarlane@strath.ac.uk

Received 25 November 2019, revised 21 January 2020
Accepted for publication 21 February 2020
Published 9 April 2020

Abstract

Recent advances in LED technology have allowed the development of high-brightness deep-UV LEDs with potential applications in water purification, gas sensing and as excitation sources in fluorescence microscopy. The emission pattern of an LED is the angular distribution of emission intensity and can be mathematically modelled or measured using a camera, although a general model is difficult to obtain and most CMOS and CCD cameras have low sensitivity in the deep-UV. We report a fluorescence-based method to determine the emission pattern of a deep-UV LED, achieved by converting 280 nm radiation into visible light via fluorescence such that it can be detected by a standard CMOS camera. We find that the emission pattern of the LED is consistent with the Lambertian trend typically obtained in planar LED packages to an accuracy of 99.6%. We also demonstrate the ability of the technique to distinguish between LED packaging types.

Keywords: Light-emitting diode, fluorescence, emission pattern, deep-ultraviolet, characterisation.

(Some figures may appear in colour only in the online journal)

1. Introduction

Recent developments in light-emitting diode (LED) technology have produced deep-ultraviolet aluminium gallium nitride (AlGaN) LEDs with wavelengths ranging between 220–280 nm emitting in the 100 mW range [1]. These LEDs have applications in sterilisation, water purification [2] and gas-sensing [3]. Deep-UV LEDs also have potential applications as excitation sources in fluorescence microscopy. In particular, 280 nm LEDs have an electroluminescence spectrum which overlaps well with the excitation spectrum of many fluorophores including semiconductor quantum dots, aromatic amino acids tryptophan and tyrosine [4] and even standard dyes such as eosin, rhodamine and DAPI [5] [6].

However, one of the major weaknesses of using deep-UV LEDs for microscopy is low transmission through glass, making deep-UV illumination sources difficult to adapt into standard epifluorescence microscopes. An alternative is to use off-axis critical illumination of the sample [7] which can also provide a shadowing effect to enhance tissue surface topography [5]. Even more simply, the LED can be used to directly illuminate the specimen without use of any lenses, but this begs the question of homogeneity of specimen illumination and hence the emission pattern of the LED in air is of interest when assessing the suitability of an LED as an excitation source in optical microscopy.

The emission pattern of an LED is the emission intensity measured as a function of angle from the normal of the LED chip [8]. In high-refractive-index planar LED chips, the refractive index change between semiconductor and air leads

to emission which follows Lambert's cosine law with radiant intensity defined by the total power of the LED divided by the surface area of a sphere of radius r surrounding the LED [9]. The intensity of light in air is described by

$$I = \frac{P_{LED}}{4\pi r^2}\frac{n_{air}^2}{n_{LED}^2}\cos(\theta), \quad (1)$$

where P_{LED} is the radiant power of the LED, r is the radius of the considered sphere, n_{air} is the refractive index of air, n_{LED} is the refractive index of the semiconductor and θ is the angle of emission measured from the normal of the LED chip. Other LED packaging geometries include hemispherical, which exhibit isotropic emission patterns, and parabolic, which have strongly directional emission patterns [9]. Some mathematical models have been developed to simulate the emission patterns of packaged LEDs and LED arrays [8, 10], however, packaged LEDs come available in different emission patterns which makes a general model difficult to obtain [8, 11]. Experimentally, the emission pattern of a visible spectrum LED can be obtained using a CCD or CMOS camera, however standard cameras are not sensitive in the deep-UV due to glass or poly-silicon elements which absorb in the UV. Back-thinned CCDs offer a solution to this problem, but are costly. Previous work studying AlGaN in LEDs has been shown to overcome these detection limits by using fluorescence to convert deep-UV radiation into visible light [12]. In this work, the authors use fluorescence to image the active region of the chip and investigate the electroluminescence distribution on the microscopic scale. Here, we apply an adaptation of this technique to a 280 nm LED in order to measure the far-field emission pattern of the LED in air. In this method, the LED is used to directly illuminate a fluorescent specimen which, due to its longer emission wavelength, can be imaged by a standard CMOS or CCD camera. The intensity across the fluorescent specimen is obtained as an indirect measurement of the emission pattern of the LED. This method is applied to measure both the intensity distribution across a 4.5 mm field of view, and, by rotating the LED about its axis, the angular emission pattern.

2. Materials and Methods

The experimental set-up to obtain the emission pattern of a 280 nm LED (LG Innotek LEUVA66H70HF00) is shown in figure 1. This model of LED has a chip size of 1 × 1 mm, a typical radiant power of 100 mW at a drive current of 350 mA and a typical viewing angle of 110°. The LED was mounted in a platform mount (Thorlabs PCM) and a 280/10 nm bandpass filter (Edmund Optics, 35–881) was placed in front of the LED to narrow the electroluminescence spectrum. A known issue with AlGaN LEDs is low-intensity visible-wavelength emission which overlaps with the emission of many fluorophores [13] – addition of an excitation filter improved spectral separation to ensure that images obtained were of the excited fluorescence only and not parasitic emission from the LED.

A fluorescent agarose block was developed using fluorescein due to its broad excitation spectrum extending into the

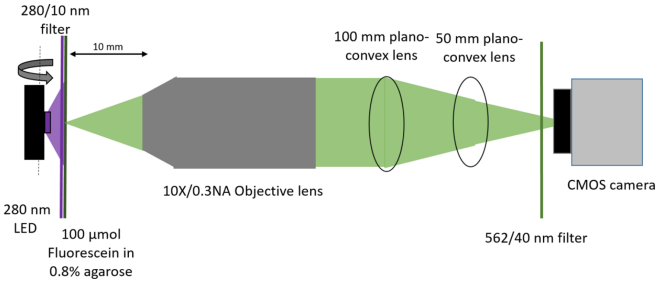

Figure 1. Experimental set up for imaging the emission pattern of a deep-UV LED. A fluorescent sample is placed in the focal plane of the objective lens and the LED is placed adjacent to the sample, behind a bandpass filter which narrows the electroluminescence spectrum of the LED. Two plano-convex lenses are employed to focus the image onto the camera chip. An emission filter is used to exclude any excitation light. To capture angular measurements, the LED was rotated about the indicated axis.

UV, high quantum yield (95% [14]) and visible peak emission wavelength of ∼520 nm. To develop the agarose block, 0.8% agarose (Sigma Aldrich 05066) was added to 100 µmol fluorescein (Sigma Aldrich F6377) in distilled water, microwaved until dissolved and pipetted into a 3D printed mould 2 mm in depth attached to a microscope slide. A path length of 2 mm was chosen in order to provide sufficient fluorescent signal. The specimen was placed in a slide holder (Thorlabs XF50) as close as possible to the LED (3.5 mm as limited by thickness of the bandpass filter).

A 10 × 0.3 NA objective lens (Olympus UPLFLN10XP) with a working distance of 10 mm was chosen to collect the fluorescence emission and the focal plane was set to the specimen. Two plano-convex lenses, 100 mm (Thorlabs LA1509-A) and 50 mm (Thorlabs LA1131-A) in focal length respectively, were used to focus the image of the fluorescent sample onto the CMOS camera (IDS UI-3060CP) with 1936 × 1216 pixels, a pixel size of 5.86 µm and a quantum efficiency of 35% at a wavelength of 400 nm (the shortest wavelength given by the manufacturer). This configuration resulted in a total magnification of 2.5×, pixel size of 2.3 µm and a field of view of 4.5 mm. An emission filter (562/40 nm, Semrock FF01-562/40-25) was placed in front of the camera.

Images were acquired at LED drive currents ranging from 50–350 mA. The resulting images were imported into Fiji [15] and background corrected by subtracting an image of the ambient light surrounding the optics. A false colour look-up table was applied to aid visualisation of the intensity distribution. An intensity line profile was taken horizontally across the field of view as this allowed measurement of a larger area due to the aspect ratio of the camera. A linewidth of 50 pixels was taken, corresponding to 116 µm, to reduce noise in the intensity profile.

The emission pattern was then measured at different angles to investigate the intensity as a function of angle. To do this, the LED was mounted on a rotating stage (Thorlabs RP01) 65 mm from the sample such that the chip lay on the axis of rotation parallel to the detector. The stage was rotated between 0° and 90° from the normal in both directions at a constant current of 350 mA and images were taken at each angle with a

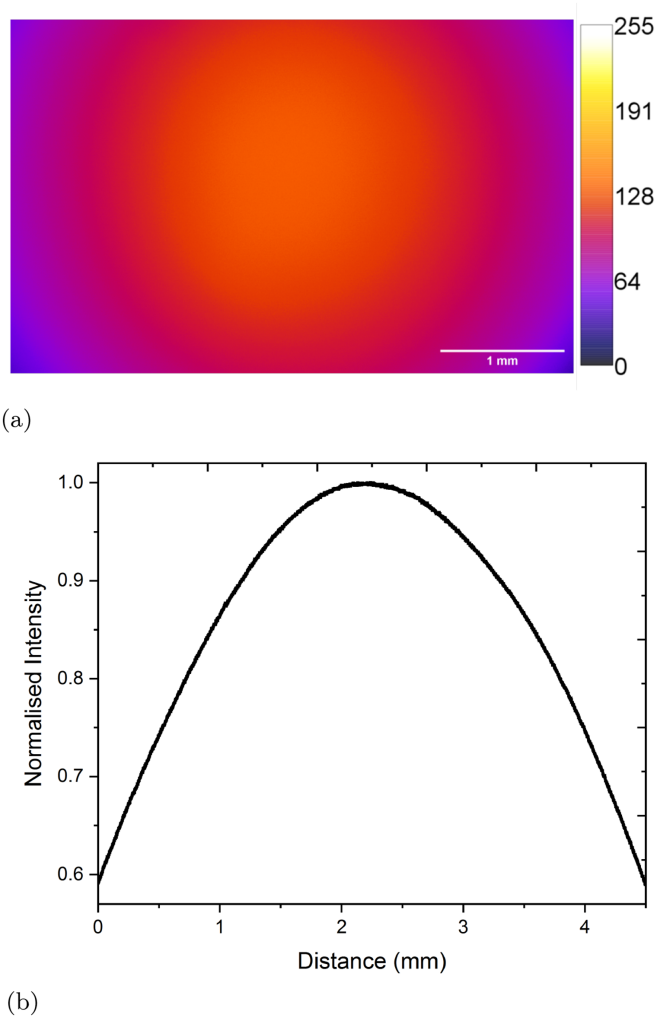

Figure 2. (a) Image of the emission pattern of a Lambertian LED taken at a drive current of 350 mA and camera exposure time of 5 ms. A false colour look-up table has been applied to aid visualisation. (b) Plot profile of above image taken horizontally across the field of view at a width of 116 μm.

longer exposure time of 50 ms to compensate for the decrease in intensity due to increased LED-sample distance. The average intensity across the image was recorded and plotted as a function of angle. An average of three images was recorded per angle. The data was fitted against a perfect Lambertian using equation (1).

To test the ability of the technique in distinguishing between types of LED packaging geometries, measurements were repeated with a second deep-UV LED specimen (Thorlabs M275D2) emitting at 275 nm which exhibits a non-Lambertian emission pattern. Images were obtained at a higher exposure time of 50 ms for static measurements and 150 ms for rotational measurements to compensate for the lower radiant power of this LED.

3. Results and Discussion

The normalised intensity distribution across the field of view of the microscope is shown in figure 2. The fluorescence

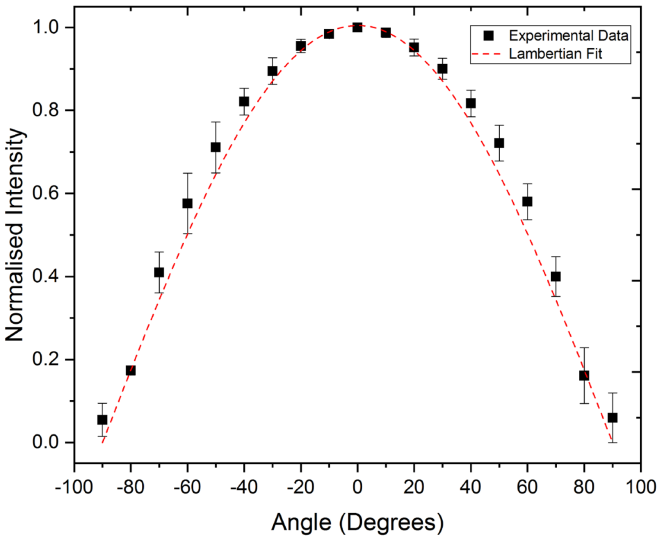

Figure 3. Emission intensity as a function of angle. The LED was rotated between 0° and 90° from the normal of the chip surface and each intensity value was recorded. Standard deviation error bars are shown on the *y*-axis and *x*-axis error bars correspond to the angular divisions on the rotating stage at ± 1°.

intensity is at its highest in the center of the field of view, reaching 60% of its maximum output at the edge. It was found that outside of changes in intensity, adjusting the drive current had no effect on the intensity distribution. Increasing the LED-specimen distance can reduce the variation in intensity as the angular distribution across the field of view becomes smaller. However, this is at the expense of the intensity of light reaching the specimen which is inversely proportional to the square of the LED-specimen distance (equation (1)).

Due to restrictions set by the field of view of the objective lens, this distribution only accounts for a small section of the LED's emission pattern (4.5 mm) which typically extends much further. To account for this, the LED can be rotated around the *x*-axis to measure the emission pattern at different incident angles. This technique allows for a broader measurement of the emission pattern of the LED and results are shown in figure 3 along with standard deviation error bars on the *y*-axis. The incident angle has a tolerance of ± 1% as limited by the scale on the rotating stage. The intensity of the fluorescence emission is at its maximum at 0° and reaches approximately 50% of its maximum value at 60° from the normal which is consistent with a Lambertian trend [9]. To test the correlation between the experimental data and a Lambertian trend, the data was fitted using equation (1) (shown in dotted lines). The data fits the Lambertian trend with a coefficient of determination of 99.6%, confirming that there is a strong correlation between the experimental data and a Lambertian trend.

Finally, a second LED specimen emitting at 275 nm with a non-Lambertian emission pattern was measured to investigate the reliability of the method to distinguish between LED types (figures 4 and 5). This LED exhibits an emission pattern towards the batwing shape, with intensity peaking at ± 20°. This result is consistent with the data sheet supplied with the

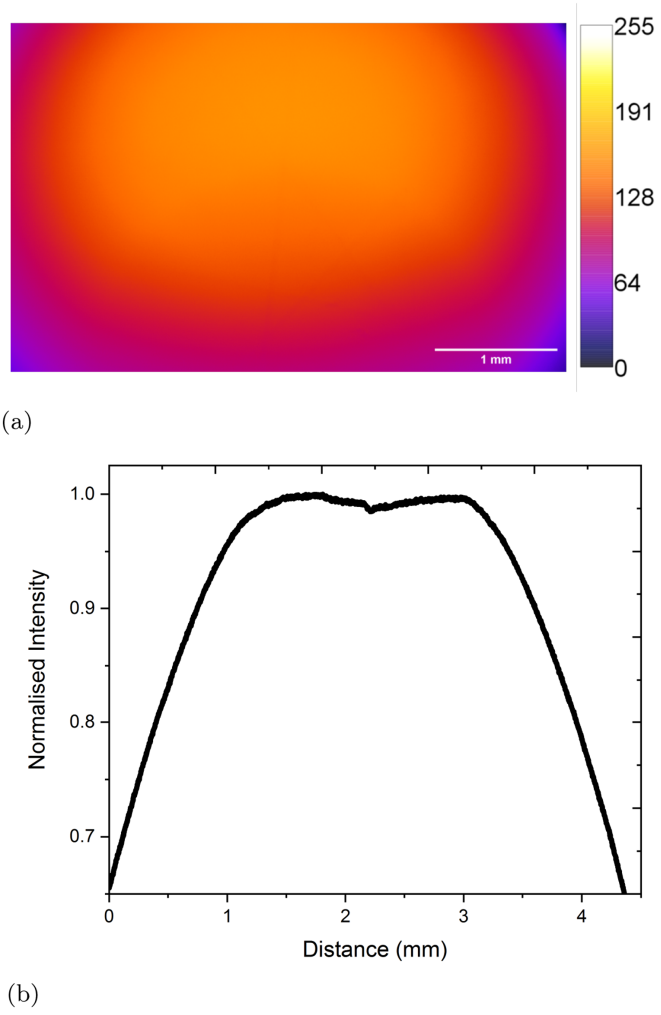

Figure 4. (a) Image of the emission pattern of a batwing LED taken at a drive current of 350 mA and camera exposure time of 50 ms. A false colour look-up table has been applied to aid visualisation. (b) Plot profile of above image taken horizontally across the field of view at a width of 116 μm.

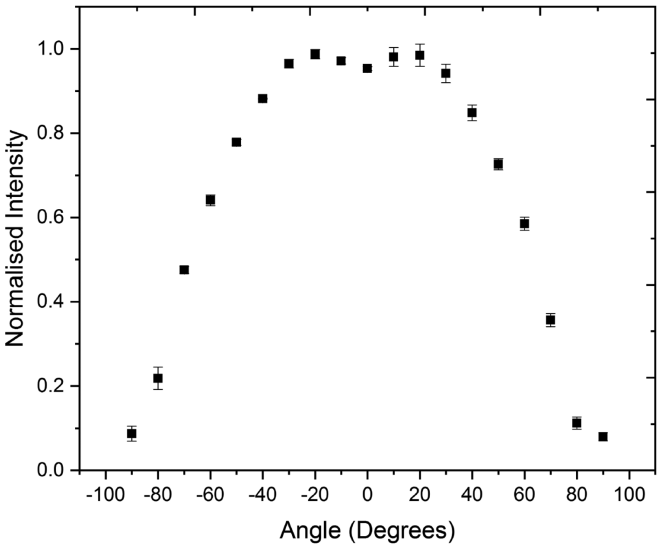

Figure 5. Emission intensity as a function of angle of a non-Lambertian emitter. Standard deviation error bars are shown on the *y*-axis and *x*-axis error bars correspond to the angular divisions available on the rotating stage at $\pm 1^{\circ}$.

LED and confirms that the technique can be used to characterise LEDs with different packaging geometries.

This is an indirect technique which lies on the assumption that fluorophores are distributed evenly across the fluorescent sample and hence changes in fluorescence intensity are directly correlated to changes in LED intensity. To test that the intensity distribution obtained was an effect of the LED itself and not the fluorescent specimen, the fluorescent specimen was rotated to compensate for any possible nonuniformity. This had no effect on the distribution obtained, confirming that the result is a property of the LED and not fluorescent specimen.

Because of the large field of view desired to measure as large an emission area as possible, the magnification was decreased to 2.5× and images were not sufficiently sampled by the camera according to the Nyquist criteria [16]. As resulting images are convolutions of the LED emission and fluorescence emission, deconvolution is desirable to revert the image to the emission of the LED only. To demonstrate this, the point spread function (PSF) of the microscope can be acquired and blind deconvolution performed to compensate for the increase in full width half maximum (FWHM) of the PSF caused by the convolution of the excitation light and fluorescent specimen. However, as Nyquist sampling could not be achieved with this set up, a diffraction limited spot would appear as a single bright pixel. To overcome this, the set up was reverted to a higher magnification by replacing the two plano convex lenses with a 200 mm tube lens, resulting in a pixel size of 416 nm which satisfies the Nyquist criteria. Sub resolution fluorescent beads (Fluoresbrite YG Microscopheres 0.5 μm, Polysciences Inc) on a quartz microscope slide were used to measure the PSF of the microscope. The image was then subjected to blind deconvolution using a Born and Wolf generated PSF (PSF Generator [17]) and a Richardson-Lucy algorithm with 10 steps (DeconvolutionLab2 [18]). The FWHM reduced from 1125.3 $\pm$ 52.8 nm to 823.1 $\pm$ 28.6 nm which, in the original set up used for measurement of the emission pattern, would be a change of less than one pixel.

Another limitation of the technique is the field of view restriction set by the objective lens which limits the detection range to 4.5 mm whilst the emission pattern of the LED is expected to be much larger. This can be overcome by rotating the LED to measure the full emission pattern, as demonstrated previously using visible spectrum LEDs [19], or scanning the LED in *x*-*y* across the field of view. For applications in optical microscopy, 4.5 mm could be considered a sufficient measurement as a typical field of view does not extend far beyond this size.

This technique could be applied to measure any wavelength of deep-UV LED due to the ability of fluorescein to become excited by wavelengths as low as 200 nm [20]. The technique could aid in the design of LED chips and LED arrays where a particular emission pattern is desired, as well as

the characterisation of packaged LEDs demonstrated here. In addition, the technique can be used to measure the homogeneity of deep-UV illumination using methods such as critical and Köhler illumination by adding the appropriate optics in the illumination pathway between LED and fluorescent specimen, as previously demonstrated using visible wavelength LEDs [21].

4. Conclusion

We have demonstrated a technique capable of measuring the emission pattern of a deep-UV LED on a camera without the requirement of UV-extended sensors. In this method, the LED is used to directly illuminate a fluorescent sample which, due to its longer emission wavelength, can be imaged by a standard CMOS or CCD camera. The intensity across the fluorescent sample is obtained as an indirect measurement of the emission pattern of the LED. The emission pattern was found to follow a Lambertian trend to an accuracy of 99.6%. The technique was successful in distinguishing between emission patterns of Lambertian and non-Lambertian emitters, confirming that the technique can allow for accurate characterisation of LEDs. The technique may also be useful in the design of LED chips or LED arrays where a particular emission pattern is required or to test the homogeneity of critical or Köhler illumination methods with deep-UV LEDs for applications in optical microscopy.

Acknowledgments

This work was supported by Medical Research Scotland (PhD-1157-2017), CoolLED Ltd and the Medical Research Council, Grant No. MR/K015583/1.

ORCID iD

Mollie McFarlane https://orcid.org/0000-0003-3921-8894

References

[1] Kneissl M, Seong T, Han J and Amano H 2019 The emergence and prospects of deep-ultraviolet light emitting diode technologies *Nat. Photon* **13** 233
[2] Song K, Mohseni M and Taghipour F 2016 Application of ultraviolet light-emitting diodes (UV-LEDs) for water disinfection: a review *Water Res* **94** 341
[3] Li J, Smeeton T M, Zanola M, Barrett J and Berryman-Bousquet V 2018 A compact breath acetone analyser based on an ultraviolet light emitting diode *Sens. Actuators* **273** 76
[4] Lacowicz J R 2004 Protein fluorescence *Principles of Fluorescence Spectroscopy* (New York: Springer Science+Business Media)
[5] Fereidouni F *et al* 2017 Microscopy with ultraviolet surface excitation for rapid slide-free histology *Nature Biomedical Engineering* **1** 957–66
[6] Guo J, Artur C, Eriksen J L and Mayerich D 2019 Three-dimensional microscopy by milling with ultraviolet excitation *Sci. Rep* **9** 14578
[7] Wong C, Pawlowski M E and Tkaczyk T S 2019 Simple ultraviolet microscope using off-the shelf components for point-of-care diagnostics *PLoS One* **14** e0214090
[8] Moreno I and Sun C C 2008 Modeling the radiation pattern of leds *Opt. Express* **16** 1808
[9] Schubert E F 2006 LED basics: optical properties *Light-Emitting Diodes* (New York: Cambridge University Press)
[10] Sheng X, Broderick L Z, Hu J, Yang L, Eshed A, Fitzgerald E A, Michel J and Kimerling L C 2011 Design and fabrication of high-index-contrast self-assembled texture for light extraction enhancement in leds *Opt. Express* **19** 703
[11] Keshavarzfathy M and Taghipour F 2019 Radiation modeling of ultraviolet light-emitting diode (UV-LED) for water treatment *J. Photochem. Photobiol* **377** 58–66
[12] Lapeyrade M *et al* 2017 Design considerations for AlGaN-based UV leds emitting near 235 nm with uniform emission pattern *Semicond. Sci. Technol* **32** 45019
[13] Liu D *et al* 2018 226 nm AlGaN/AlN UV LEDs using p-type Si for hole injection and UV reflection *Appl. Phys. Lett* **113** 011111
[14] Lacowicz J R 2004 Quantum Yield Standards *Principles of Fluorescence Spectroscopy* (New York: Springer Science+Business Media)
[15] Schindelin J, Arganda-Carreras I and Frise E *et al* 2012 Fiji: an open-source platform for biological-image analysis *Nat. Methods* **9** 676
[16] Pawley J B 2006 Points, pixels and gray levels: Digitizing image data *Handbook of Biological Confocal Microscopy* (New York: Springer Science+Business Media)
[17] Kirshner H, Aguet F, Sage D and Unser M 2013 PSF fitting for fluorescence microscopy: Implementation and localization application *J. Microsc* **249** 13–25
[18] Sage D, Donati L, Soulez F, Fortun D, Schmit G, Seitz A, Guiet R, Vonesch C and Unser M 2017 Deconvolutionlab2: An open-source software for deconvolution microscopy *Methods* **115** 28–41
[19] Manninen P, Hovila J, Karha P and Ikonen E 2007 Method for analysing luminous intensity of light-emitting diodes *Meas. Sci. Technol* **18** 223–9
[20] Gutierrez D, Alvarez J and Racedo F 2019 Development of a steady-state fluorescence spectroscopy system and a time-resolved fluorescence spectroscopy system *Conf. Series: Journal of Physics: Conf. Series* **1247** 012017
[21] Bosse J B, Tanneti N S, Hogue I B and Enquist L W 2015 Open led illuminator: A simple and inexpensive LED illuminator for fast multicolor particle tracking in neurons *PLoS One* **10** e0143547